Chemical Physics 411 (2013) 17–25

Contents lists available at SciVerse ScienceDirect

Chemical Physics

journal homepage: www.elsevier.com/locate/chemphys

Electronic transitions in a series of 2-azaazulene polymethine dyes with different π-conjugation lengths

Olga V. Przhonska [a,b], Honghua Hu [a,*], Scott Webster [a], Julia L. Bricks [c], Alexander A. Viniychuk [c], Alexey D. Kachkovski [c], Yuriy L. Slominsky [c]

[a] CREOL and FPCE, The College of Optics and Photonics, University of Central Florida, Orlando, FL 32816, United States
[b] Institute of Physics, National Academy of Sciences, Prospect Nauki 46, Kiev 03028, Ukraine
[c] Institute of Organic Chemistry, National Academy of Sciences, Murmanskaya 5, Kiev 03094, Ukraine

ARTICLE INFO

Article history:
Received 13 August 2012
In final form 26 November 2012
Available online 7 December 2012

Keywords:
Polymethine
2-Azaazulenes
π-Conjugated chain
Terminal groups
Symmetry breaking
Wave of charge
Bond length alternation
Quantum chemical calculations
Localized and delocalized molecular orbitals

ABSTRACT

A comprehensive quantum chemical analysis along with spectral-luminescence measurements has been performed for a new series of 2-azaazulene dyes with different conjugation lengths (n) to better understand the nature of their electronic transitions. The remarkably large red shift of their main absorption bands at relatively small n is connected with the existence of totally delocalized HOMO and LUMO. Symmetry breaking is observed experimentally at $n = 3$ in polar solvents and theoretically at $n = 5$ in vacuum. Analysis shows the existence of two types of molecular orbitals (MOs): local with the charge mainly localized within the terminal groups, and delocalized with the charge distributed throughout the molecule. Correspondingly, three types of electronic transitions are present: between delocalized MOs; between one local and one delocalized MO, and between local MOs only, which is important for predicting the positions of electronic transitions to the chain length.

1. Introduction

Polymethine dyes (PDs) have been studied for more than a century, however, they continue to be actively investigated due to their multifunctional chemical, biological and optical applications (reviews [1–3] and references therein). The most essential advantages of PDs are connected with their intense (with molar absorbance up to $3 \times 10^5\ M^{-1}\ cm^{-1}$) and tunable absorption bands in the visible and near infrared (NIR) regions, which is important for the development of organic materials with large third-order nonlinearities for all-optical signal processing [4–7]. The electronic properties of these dyes can be modified by changing the conjugation chain length or by adding specific terminal groups of electron acceptor (A) or electron donor (D) nature. There are two generally accepted synthetic methods to shift the absorption bands to the NIR region and, correspondingly, to decrease the energy gap between the ground and excited states: (1) lengthening the π-conjugated chain and (2) introduction of terminal groups with their own π-electron systems which can increase the total length of conjugation by adding the contribution of the terminal group to the polymethine chain [3]. The first typically results in a decrease of thermal and photochemical stability of the extended compound, while the second allows shifting the absorption peak to the "red" without a significant decrease of their photostability. As was shown earlier, one of the largest "red" shifts in the peak absorption was obtained in a PD by incorporating dihydrobenzo[cd]furo[2,3-f]indolium terminal groups [8,9]. We demonstrated the effect of these terminal groups is equivalent to the extension of the polymethine chain to 3 vinylene groups. The development of terminal groups that strongly interact with the polymethine chromophore and, thus, shift the absorption bands to the NIR region is practically important. In addition, our interest in the study of NIR dyes is determined by numerous remaining theoretical questions connected with the specific features of the conjugated systems absorbing in the range $\geqslant$1000 nm. The most important issues are the following: (1) Extensive broadening of the absorption bands in polar solvents explained by symmetry breaking and reduced charge delocalization within the polymethine chromophore [10–14]. However, there is still a lack of detailed experimental data along with their theoretical interpretation; (2) Understanding the origin of charge localization and delocalization within specific molecular orbitals and their effect on the nature of the electronic transitions; and (3) Understanding the role of π-conjugation in the terminal groups and their interaction with the conjugation chain in shifting of absorption bands into the "red" region.

* Corresponding author.
E-mail address: honghua@creol.ucf.edu (H. Hu).

0301-0104/$ - see front matter © 2012 Elsevier B.V. All rights reserved.
http://dx.doi.org/10.1016/j.chemphys.2012.11.017

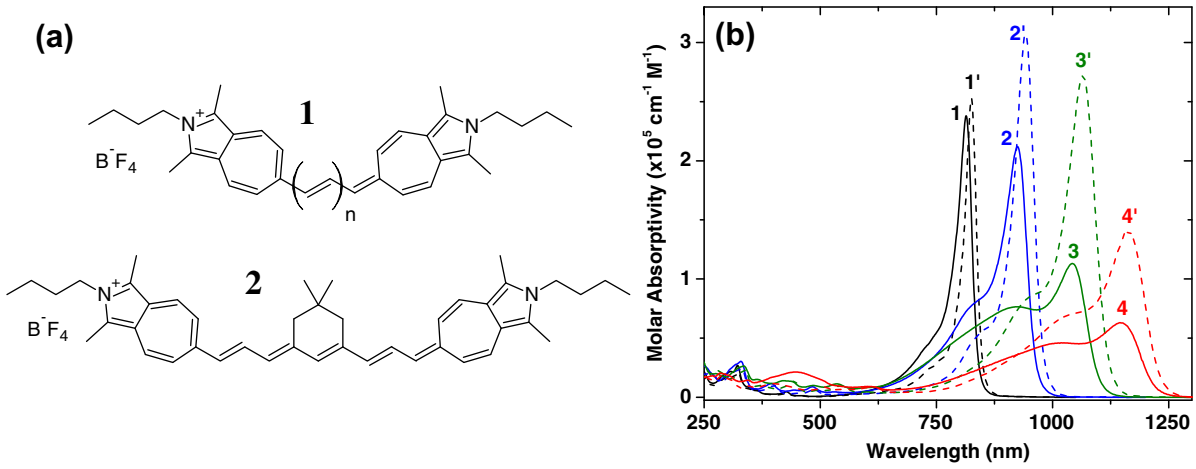

Fig. 1. (a) Molecular structures of JB7-08 (**1**, $n = 1$), JB9-08 (**1**, $n = 2$), JB17-08 (**1**, $n = 3$), and JB5–09 (**2**, $n = 4$); (b) Linear absorption spectra of JB7-08 (1, 1'), JB9-08 (2, 2'), JB17-08 (3, 3'), and JB5-09 (4, 4') in ACN (1, 2, 3, 4) and DCM (1', 2', 3', 4').

We believe that finding the answers to these questions will stimulate further development of the quantum chemical theories which, as is well known, have many limitations in the description of NIR dyes [15,16]. In an attempt to better understand these molecules and answer some of the above questions, we synthesised and studied a series of cationic polymethines with 2-azaazulene (cyclohepta-[*c*]pyrrole) or pseudoazulene terminal groups, which are characterized by their own extended π-conjugated system strongly connected to the conjugated system of the chain. We show that these heterocycles are characterized by a large "effective conjugation length" and are good prospects for the synthesis of NIR dyes as they provide intense NIR absorption at relatively short chain lengths. The distinguishing feature of these terminal groups is that they are chemically symmetric relative to the axis drawn through two atoms of each terminal residue: the nitrogen and carbon atom connected with the polymethine chain, see the chemical structure presented in Fig. 1(a). This structural feature allows us to separate delocalized molecular orbitals with the charge distributed within the whole molecule from the local orbitals with the charge localized within terminal groups only.

In this paper we present the results of a combined spectral-luminescence investigation and quantum chemical analyses of a series of symmetrical polymethine dyes containing 2-azaazulene (cyclohepta-[*c*]pyrrole) terminal groups and different π-conjugation lengths with the goal of understanding the nature of their electronic transitions. The result of this research is moving us closer to the ultimate goal of understanding structure–property design strategies and developing a predictive capability for the nonlinear optical properties of linear conjugated molecules.

2. Experimental methods and results

2.1. Materials characterization

The molecular structures of the dyes studied in this paper are shown in Fig. 1(a). They are: 2-butyl-6-[3-(2-butyl-1,3-dimethylcyclo-hepta[*c*]pyrrol-6(2H)-ylidene)prop-1-en-1-yl]-1,3-dimethylcyclohepta[*c*]pyrrolium tetrafluoroborate (labeled as JB7-08); 2-butyl-6-[5-(2-butyl-1,3-dimethylcyclo-hepta[*c*]pyrrol-6(2H)-ylidene) penta-1,3-dien-1-yl]-1,3-dimethylcyclohepta[*c*]pyrrolium tetrafluoroborate (labeled as JB9-08); 2-butyl-6-[7-(2-butyl-1,3-dimethylcyclo-hepta[*c*]pyrrol-6(2H)-ylidene)hepta-1,3,5-trien-1-yl]-1,3-dimethylcyclohepta[*c*]pyrrolium tetrafluoroborate (labeled as JB17-08); 2-butyl-6-((1*E*,3*E*)-4-{(3*E*)-3-[2-(2-butyl-1,3-dimethylazulen-6(2*H*)-ylidene)ethylidene]-5,5-dimethylcyclohex-1-en-1-yl} buta-1,3-dien-1-yl)-1,3-dimethylcyclohepta[*c*]pyrrolium tetrafluoroborate (labeled as JB5-09). These dyes differ by the length of polymethine chromophore from $n = 1$ for JB7-08 to $n = 4$ for JB5-09, where n is the number of vinylene groups in the chain. The corresponding tetracarbocyanine JB5-09 (structure **2** in Fig. 1(a)) includes a six-membered cycle (trimethylene bridge) in the polymethine chromophore to increase its thermal and photostability.

2.2. Synthesis

All starting materials and solvents for the dye synthesis are supplied by Aldrich and used without further purification. Melting points (mp) are measured by Kleinfeld GmbH measurement apparatus and are uncorrected. All NMR measurements are carried out on a Varian GEMINI 2000 spectrometer with 1H frequencies of 400.07 MHz at room temperature. Tetramethylsilane was used as a standard for chemical shift scale calibration. ^{1}H NMR spectra were recorded with a spectral width of 8000 Hz and number of points equaling 32,000. All compounds are recrystallized before use, and their structures were confirmed by NMR analysis.

The syntheses of JB7-08 and JB9-08 have been reported previously [17–19]. The symmetrical trimethine cyanine (JB7-08) and pentamethine cyanine (JB9-08) have been synthesised by the reaction of 2-butyl-1,3,6-trimethylcyclohepta[*c*]pyrrolium tetrafluoroborate with triethyl orthoformate in the first case, or with N-(3-anilinoprop-2-en-1-ylidene)benzenaminium chloride in the second case in acetic anhydride in the presence of anhydrous sodium acetate. JB17-08 has been synthesised analogically from 2-butyl-1,3,6-trimethyl-cyclohepta[*c*]pyrrolium tetrafluoroborate (0.315 g, 1 mM) and N-(5-anilino-2,4-pentadien-1-ylidene)benzenaminium chloride (0.140 g, 0.5 mM) with a yield of 0.1 g (%) and a melting point of 149–150 °C (decomposition). The synthesis of JB5–09 has been performed from 2-butyl-1,3,6-trimethyl-cyclohepta[*c*]pyrrolium tetrafluoroborate (0.315 g, 1 mM) and N-(2-{3-[2-anilinovinyl]-5,5-dimethyl-2-cyclohexen-1-ylidene} ethylidene) benzenaminium chloride (0.189 g, 0.5 mM). Yield 0.120 g (%), mp > 220 °C. Calcd. for C44H55BF4N2 (698.44): C 75.63, H 7.97, N 4.01%; found: C 75.38, H 7.62, N 4.37%.

2.3. Spectral-luminescence properties

The linear absorption spectra of all molecules in two solvents of different polarity are recorded by a Varian Cary 500 spectrophotometer and presented in Fig. 1(b). The concentrations of the solutions are kept below 10^{-5} M, further dilution does not lead to any change of the shape of the absorption spectra, i.e. no indication of aggregation is observed below 10^{-5} M. The choice of solvents is

based on the solubility of the dyes and the solvent polarity (or orientational polarizability) given by $\Delta f = (\varepsilon - 1)/(2\varepsilon + 1) - (n^2 - 1)/(2n^2 + 1)$, where ε is the static dielectric constant and n is the refractive index of the solvent [20]. Calculated Δf values range from 0.217 for dichloromethane (DCM) to 0.306 for acetonitrile (ACN). Dyes cannot be dissolved in solvents of lower polarity. Absorption spectra of all dyes are composed of intense cyanine-like bands attributed to the $S_0 \rightarrow S_1$ absorption, with the main absorption peaks shifted by ≈100 nm to longer wavelengths upon lengthening of the main conjugation chain from $n = 1$ to $n = 4$, and weak linear absorption in the visible and UV region corresponding to absorption to higher excited states, $S_0 \rightarrow S_n$. The first dye from this series, JB7-08 ($n = 1$), with the absorption peak at 825 nm in DCM, exhibits classical nonpolar solvatochromism, indicating a symmetrical ground and excited state charge distribution and small permanent dipole moments, 1–2 D, oriented perpendicular to the polymethine chromophore [10]. In contrast, absorption spectra of the dyes JB17-08 and especially JB5-09, placed in the range of ⩾1000 nm, demonstrate a substantial band broadening in polar ACN represented by the growth of the short wavelength shoulder. Note that JB5-09 demonstrates band broadening in both solvents. This is a strong indication of polar solvatochromism which is typical for dyes that exhibit ground-state charge localization and a large ground-state permanent dipole moment. This effect was investigated by us earlier theoretically [5,21] and experimentally [8,10] and explained by a ground state *symmetry breaking* leading to the appearance of a molecular form with an asymmetrical charge distribution and, as a result, with an asymmetrical bond-length alternation. In our theoretical paper, see Ref. [5], we show that the minimum number of vinylene groups, n, necessary to break the symmetry of the simple streptocyanine molecule, is eight in the gas phase and six in nonpolar cyclohexane. An increase in the solvent polarity results in a decrease of n. An additional absorption at the shorter wavelength region (under the vibrational shoulder) corresponds to a molecular geometry with charge localized at one of the molecular terminal groups that is additionally stabilized by the solvent. Thus, our results demonstrate the possibility of the coexistence of the two forms in polar solvents leading to absorption band broadening.

It is important to note that all 2-azaazulene dyes show a remarkably large red shift of their main absorption bands at relatively short polymethine chain lengths. Even the shortest dye from this series, JB7-08 (with $n = 1$), shows an absorption peak at 825 nm, which is ≈270 nm longer than traditional polymethine dyes with indolium or thiazolium terminal groups and the same chain length [22]. Thus, the effect of these terminal groups is equivalent to the extension of the polymethine chain to approximately 3 vinylene groups, only slightly smaller (at ≈40 nm) than the effect of dihydrobenzo[cd]furo[2,3-f]indolium terminal groups, studied by us earlier [8]. Detailed quantum-chemical analysis is presented in Section 3.

The fluorescence spectra, corrected for the spectral responsivity of the detection system, are measured by a PTI QuantaMaster spectrofluorimeter. Fluorescence quantum yield, η, is measured in comparison with the standard dyes, Cresyl Violet in methanol ($\eta = 0.54$) and polymethine dye PD 2631 or 3-ethyl-2-[7-(3-ethyl-1,1-dimethyl-1,3-dihydro-2H-benzo[e]indol-2-ylidene) hepta-1,3,5-trienyl]-1,1-dimethyl-1Hbenzo[e]indolium-4-methylbenzenesulfonate ($\eta = 0.11$) which has been proposed by us as a fluorescence standard near 800 nm [7]. For JB7-08, with the shortest polymethine chain, the fluorescence quantum yield is extremely small in both solvents ($\eta < 0.001$). Small, however, measurable quantum yields, $\eta \approx 0.05$, are obtained for JB9-08 and JB17-08 supporting short fluorescence lifetimes, τ_F, of their first excited states, based on the calculations using Strickler–Berg equation [23]. We also directly measured the fluorescence lifetime of JB17-08 by a femtosecond pump–probe technique [7] and obtained the value of $\tau_F = 28 \pm 2$ ps. Fluorescence spectra, shown in Fig. 2(a) for JB17-08 in DCM and ACN, are relatively narrow and independent of the solvent polarity, confirming that the emission occurs only from the symmetrical form, in accord with previous measurements for other dyes with the symmetry-broken geometry [8]. No fluorescence was observed for the longest dye JB5-09. Its chemical instability complicates spectral-luminescence measurements and requires special control of the absorption contour during the measurements.

We note that JB7-08 (with $n = 1$) does not emit from the first excited state S_1, but has a weak fluorescence from a higher lying excited state, so called "blue" fluorescence $S_n \rightarrow S_0$, which is in the range of 450–600 nm. "Blue" fluorescence at the same spectral range was also observed for JB17-08 (see Fig. 2(b)). This unusual effect was previously observed in another series of polymethine dyes with "heavy", branched terminal groups [8]. Great care in purification of the dye powders was taken to insure the validity of this "blue" fluorescence and to understand the origin of this emission.

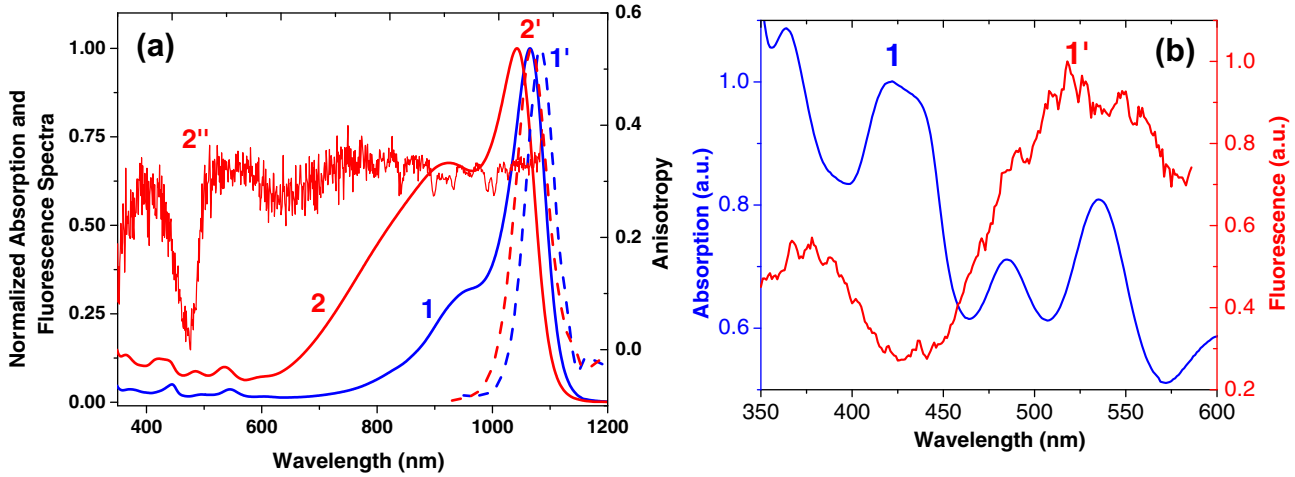

Fig. 2. (a) Linear absorption (1,2), fluorescence (1',2') and excitation anisotropy (2'') spectra of JB17-08 in DCM (1,1'), and ACN (2,2',2''); (b) Linear absorption in the range 350–600 nm (1) and "blue" fluorescence (1') of JB17-08 in ACN. (For interpretation of the references to colour in this figure legend, the reader is referred to the web version of this article.)

2.4. Anisotropy measurements

The relatively short fluorescence lifetimes of JB7-08 and JB17-08, as compared to the rotational reorientation times of the molecules in ACN and DCM (typical values of 350–450 ps [24]), allow a direct measurement of the anisotropy spectra without use of a viscous solvent. The excitation anisotropy spectrum for JB17-08 in ACN, obtained by fixing the emission wavelength at the peak of the main $S_1 \rightarrow S_0$ fluorescence band, is presented in Fig. 2(a). The anisotropy value $r(\lambda)$ for a given excitation wavelength λ can be calculated as: $r(\lambda) = \frac{I_{||}(\lambda) - I_{\perp}(\lambda)}{I_{||}(\lambda) + 2I_{\perp}(\lambda)}$ where $I_{||}(\lambda)$ and $I_{\perp}(\lambda)$ are the intensities of the fluorescence signal polarized parallel and perpendicular to the excitation light, respectively [20]. For JB17-08 in ACN this spectrum is relatively noisy as a result of its small fluorescence efficiency ($\eta \approx 0.05$). However, this spectrum is important to locate the positions of forbidden $S_0 \rightarrow S_n$ transitions, for example, transitions between states of the same symmetry. These forbidden transitions are too weak to be observed in linear absorption measurements. As seen from Fig. 2(a), the anisotropy spectrum is flat within the main absorption band (up to ≈750 nm) and $r(\lambda)$ values are high (≈0.35) indicating a small angle between the absorption and emission transition dipoles. The decrease in the values of $r(\lambda)$ in the range from 700 nm to 550 nm locates the position of the next electronic state (or group of states) with a larger angle (≈30°) between the absorption and emission transition dipoles. The deepest valley is observed in the range 430–470 nm indicating an angle up to 65° between these two dipoles. Information obtained from anisotropy measurements combined with quantum chemical calculations allows a deeper understanding of the nature of electronic transitions.

Linear spectroscopic measurements allow the calculation of the values for the transition dipole moments, μ_{01}, as: $\mu_{01} = \sqrt{\frac{1500(\hbar c)^2 \ln(10)}{\pi N_A E_{01}} \int \varepsilon_{01}(\nu) d\nu}$, where $\varepsilon_{01}(\nu)$ is the molar absorbance, N_A is Avogadro's number, and E_{01} is the energy at the absorption peak [20] in CGS units. Calculations, based on linear absorption in low polarity DCM, give the following values for the main absorption bands: 12 D for JB7-08, 15.6 D for JB9-08, 18 D for JB17-08 and 16 D for JB5-09.

3. Quantum chemical analysis

Quantum chemical orbital analysis is performed with the goal of understanding the formation of the linear absorption spectra in the vinylogous series of NIR dyes with 2-azaazulene (cyclohepta-[c]pyrrole) terminal groups and their structure–property relations. Calculations are performed for the series of dyes with n = 1–5 in vacuum. For simplicity, all molecular structures are considered with the open polymethine chains without bridges. As was shown by us earlier, cyclization of the part of the chain by a six-membered (trimethylene) bridge does not cause considerable distortion of the ground state geometry as compare to unsubstituted chromophore [25].

Ground state geometry optimization is performed by *ab initio* method (RHF/6-31G**) using the standard program package Gaussian 2003 [26]. The electronic transitions are calculated by semi-empirical ZINDO/S and, for comparison, by TD DFT methods. Both methods give a considerable divergence between calculated and experimental data of the electronic transitions (up to 0.4 eV in ZINDO/S and 0.7 eV in TD DFT for the $S_0 \rightarrow S_1$ transitions, and much smaller for the higher transitions). This limitation of quantum chemical theories is known for the long linear conjugated systems, especially PDs absorbing in the NIR spectral region [15,16]. However, this inaccuracy is smaller than the energy difference between electronic transitions analyzed in our paper, therefore both methods give the same order of the molecular orbitals (MOs) and charge distributions resulting in the same order and nature of the electronic transitions. Based on this information and performing a direct comparison with the experimental spectral properties, we suppose that we are able to analyze correctly the nature of the electronic transitions in a homological series of dyes.

3.1. Ground state geometry optimization

The calculations of the optimized molecular geometries by *ab initio* method (RHF/6-31G**) for 2-azaazulenes with n = 1–5 show that all molecular structures are planar without any spatial hindrances between the terminal groups. Owing to symmetrical constitution of the terminal groups, their 180° rotation does not lead to a formation of energetically different structures: all possible rotational conformers are identical. Our quantum chemical calculations clearly show that only all-trans-form is the most energetically preferable in the ground state at room temperature as the energy barriers for formation of other types of isomers (including rotation around the bonds placed in the middle of the chain) are much larger than kT. Additionally we performed calculation of the spectral positions and oscillator strengths for the electronic transitions in possible cis-forms. We found that the spectral peaks of the $S_0 \rightarrow S_n$ transitions in cis-isomers differ on several nanometers only from the corresponding transition peaks in trans-form. Therefore, a broad shoulder in the absorption spectrum in polar ACN cannot be connected with $S_0 \rightarrow S_1$ transition in the cis-form. It also cannot be connected with $S_0 \rightarrow S_2$ transition in the cis-form as oscillator strength of this transition remains small and contradicts the experimentally measured anisotropy spectrum.

The calculated CC bonds within the chain are practically equalized for all 2-azaazulene dyes with n = 1–4 and equal to ≈1.4 Å, typical CC bond length for polymethine chromophore [27–29]. Some bond length alternation (BLA) is observed within the terminal azaazulene heterocycles similar to the initial azaazulene salt (studied in Ref. [17]). The valence angles between CC bonds in the chain are equal ≈123–125°, somewhat larger than a typical value of 120° known for the conjugated chain of carbon atoms with sp^2 hybridization. The valence angles within the 2-azaazulene terminal groups are larger in 7-membered cycle (≈130°) and smaller in 5-membered cycle (≈108°) as compare to the chain angles.

Calculations show that for 2-azaazulene dye with n = 5 the optimized molecular geometry drastically changes: there is a considerable BLA along the polymethine chain increasing from one terminal group to another. Similar BLA is typically observed for nonsymmetrical polymethine dyes with the different terminal groups, where alternation is escalating from the terminal group with the higher donor ability to the terminal group with the smaller donor ability [30]. Thus, the appearance of the BLA for the dye with n = 5 is a sign of the symmetry breaking effect. Note that the introduction of a trimethylene bridge to the polymethine chain does not protect the dye structure from ground state symmetry breaking. Our calculations show that BLA and asymmetrical charge distribution are similar in both dyes (with and without trimethylene bridges) at n = 5.

In contrast to quantum chemical calculations showing the appearance of symmetry breaking at n = 5, our experimental results demonstrate that in the polar solvents symmetry breaks earlier, at n = 3. Absorption spectrum shown in Fig. 1(b) for the dye JB17-08 clearly reveals a coexistence of the forms with the symmetrical and asymmetrical charge distribution and bond length equalization and alternation, correspondingly, similar to results previously reported for thiapentacarbocyanine dye in Ref. [10]. It is important to note that quantum chemical calculations for all 2-azaazulene dyes with $n \geqslant 5$ give only asymmetrical molecular geometry with BLA, as the most energetically preferable form.

Therefore, in order to theoretically analyze the properties of the symmetrical form at the same chain length $n \geqslant 5$, we perform the following procedure. Using the optimized molecular geometry of the previous vinilog with $n = 4$ (without BLA), we are constructing a longer chain by introducing of two additional CH-groups to the chain center. In the obtained molecule with $n = 5$, we perform a correction of CC bond lengths within the chromophore based on the trend analysis of the changes in the bond lengths upon the lengthening of the chain.

3.2. Molecular orbital analysis

It is shown earlier that the donor terminal groups in D-π-D symmetrical polymethine molecules can significantly affect the positions and charge distribution of the highest occupied molecular orbitals (HOMOs) [31]. These two orbitals, which can be called *donor orbitals*, are formed by the mixing, interaction and splitting of the HOMOs of both terminal residues and HOMO of the conjugated chain. Fig. 3 schematically represents the formation of MOs in the 2-azaalulene dye with $n = 1$ (structure **1**, Fig. 1(a)) based on the energy positions and charge distribution of the MOs in the terminal groups (or initial salt) and MOs of the polymethine chain of corresponding length. Due to the symmetrical constitution of the 2-azaazulene donor terminal groups, their HOMOs, shown in Fig. 3(a) and (c), have nodes at the carbon atoms connecting these terminal groups with the polymethine chain. Therefore, they cannot interact with the HOMO of the chain (Fig. 3(b)). As a result, two degenerate orbitals are formed in the dye molecule, HOMO−1 and HOMO−2, which can be called *local MOs*, as shown in Fig. 3(d). The next MO of each residue, HOMO−1, can interact with the chain due to the absence of the molecular node in the corresponding position. This interaction leads to a large splitting of orbitals and formation of two *donor orbitals*, HOMO (anti-symmetrical) and HOMO−3 (symmetrical) in the dye molecule. This large splitting of *donor orbitals* leads to the *local MOs* (HOMO−1 and HOMO−2) specifically placed between HOMO and HOMO−3 as shown in Fig. 3(d). These factors result in a substantial shift of HOMO in dye molecule (as shown in Fig. 3(d)), thus decreasing HOMO–LUMO interval. Therefore, 2-azaazulene dyes show a remarkable large red shift of their absorption bands.

Lowest unoccupied molecular orbital, LUMO, in the dye molecule represents a level of the charge and originates from LUMO of the chain, which is typical for all cationic dyes [31]. Two LUMOs of both terminal groups, having the antinodes at the positions of their connection with the polymethine chain, can interact with the chain resulting in a formation of two *delocalized orbitals*, LUMO+1 (anti-symmetrical) and LUMO+4 (symmetrical), as shown in Fig. 3(d). In contrast, two LUMO+1 orbitals of both terminal groups, having the nodes at their connection with the polymethine chain, form two *local MOs* in the dye molecule, LUMO+2 and LUMO+3, placed between *delocalized orbitals*.

Based on the origin of charge distribution, we can conclude that there are two types of molecular orbitals in the 2-azaazulene molecules: *local MOs* with the charge mainly localized within terminal groups and *delocalized MOs* with the charge distributed within the whole molecule. Among *delocalized orbitals*, especially important are two *donor orbitals* (HOMO and HOMO−3), whose energy positions are determined by donor strength of the terminal groups.

Table 1 represents the calculated (ZINDO/S, Gaussian 2003) energy positions (in eV) of the MOs in the vinylogous series of 2-azaazulene dyes with $n = 1$–5. As can be seen from Table 1, occupied *local orbitals* are: HOMO−1 and HOMO−2 for the dyes with $n = 1$–3, and HOMO−2 and HOMO−3 for dye with $n = 4$ and for symmetrical form with $n = 5$. Unoccupied *local orbitals* are: LUMO+2 and LUMO + 3 for the dyes with $n = 1$–4, and LUMO+3 and LUMO+4 for symmetrical form with $n = 5$. Obviously, no degenerate MOs are observed for asymmetrical form with $n = 5$. Fig. 4 represents the shapes and positions of MOs for 2-azaalulene dye with $n = 5$. As was mentioned above, calculations give a symmetry-broken geometry (Fig. 4(b)) as the most preferable molecular structure. The symmetrical form for this dye (Fig. 4(a)) was constructed by procedure described in Section 3.1. It is seen that degeneracy is removed for asymmetrical form, however, charge distribution can still be considered as localized at one of the terminal group.

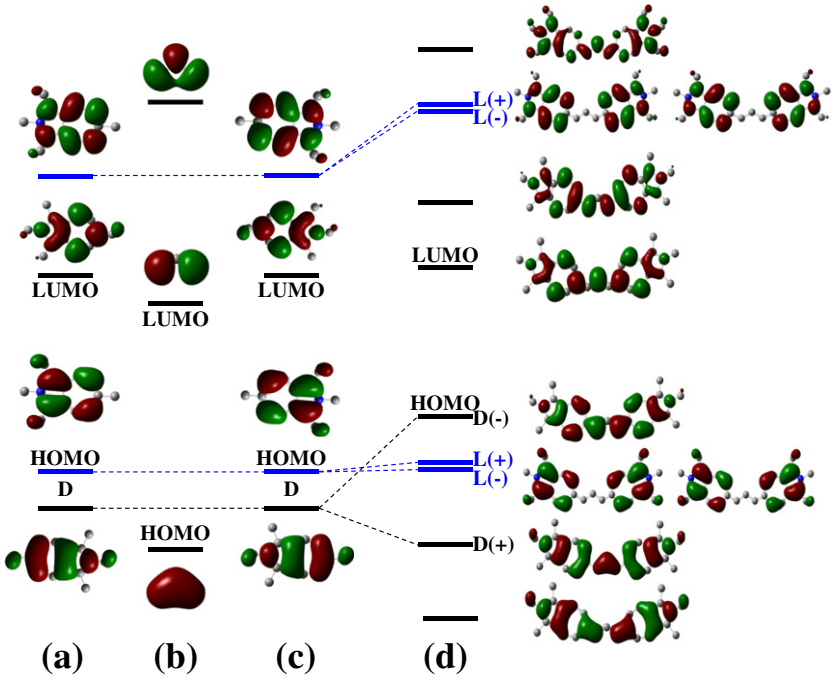

Fig. 3. Schematic of formation of MOs in 2-azaalulene dye **1** with $n = 1$ (d) from MOs of the terminal groups (a) and (c) and the chain (b). *Local* orbitals (L) are shown in blue; *delocalized* orbitals (D) are shown in black. (For interpretation of the references to colour in this figure legend, the reader is referred to the web version of this article.)

Table 1
Energies (in eV) of the molecular orbitals (MOs) in 2-azaazulenes with $n = 1–5$; $n = 5$ s and $n = 5$as correspond to symmetrical (s) and asymmetrical (as) molecular structures. *Italic* numbers indicate the degenerate (*local*) MOs. ZINDO/S calculations, Gaussian 2003.

Mos	$n = 1$	$n = 2$	$n = 3$	$n = 4$	$n = 5$ s	$n = 5$ as
LUMO+4	2.421	2.095	1.687	1.333	*1.142*	2.231
LUMO+3	*0.653*	*0.816*	*1.006*	*1.170*	*1.115*	1.061
LUMO+2	*0.598*	*0.789*	*0.979*	*1.088*	0.762	0.272
LUMO+1	0.163	−0.163	−0.435	−0.571	−0.979	−0.462
LUMO	−2.531	−2.530	−2.476	−2.476	−2.448	−2.639
HOMO	−8.925	−8.489	−8.190	−7.972	−7.482	−7.700
HOMO−1	*−9.877*	*−9.741*	*−9.578*	−9.415	−9.006	−8.653
HOMO−2	*−9.877*	*−9.741*	*−9.578*	*−9.496*	*−9.415*	−9.252
HOMO−3	−11.292	−10.612	−9.986	*−9.523*	*−9.415*	−10.122
HOMO−4	−12.707	−12.136	−11.562	−11.020	−10.530	−10.585

3.3. Bond length alternation

It is known that BLA, representing a difference between the neighboring CC bonds, can be characterized by Δl_v function: $\Delta l_v = (-1)^v(l_v - l_{v+1})$, where l_v is a length of the v-th carbon bond [11]. This parameter Δl_v can be used for characterization of the shape and location of the BLA wave (also called as geometrical soliton [11]). Sometimes, it is convenient to describe these waves by their modulus (or scalar values): $|\Delta l_v| = |l_{v+1} - l_v|$. The calculated BLA functions (*ab initio*, RHF/6-31G**) for a series of azaalulene dyes with $n = 1–5$ are presented in Fig. 5.

It is seen that the difference in the bond lengths is minimal in the center of the chromophore, however the lengthening of the polymethine chain is accompanied by a small but regular increase of the $|\Delta l_v|$ function near the terminal groups. Calculations indicate a significant degree of BLA within the heterocyclic terminal groups, which is similar to all dyes in this series. In contrast to symmetrical structure with $n = 5$, its asymmetrical form shows a considerable BLA along the polymethine chain increasing from one terminal group to another. Similar BLA is typically observed for the dyes with the different terminal groups, and in this case $|\Delta l_v|$ function increases from the terminal group with the higher donor ability to the group with the lower donor strength [30].

3.4. Charge distribution in the ground and the first excited states

It is well known that all polymethine dyes are characterized by a considerable alternation of the charge magnitudes at neighboring carbon atoms within the conjugated chain [30]. For symmetrical 2-azaazulene dyes with $n = 1–3$ it is confirmed by us experimentally with ^{13}C NMR spectroscopy. Similar to the BLA function, the difference of the electron densities at the neighboring carbon atoms μ and $\mu + 1$ can be characterized by charge alternation function Δq_μ, which can be calculated as: $\Delta q_\mu = (-1)^\mu(q_\mu - q_{\mu+1})$, where q_μ is traditional Mulliken atomic electron density [12]. This parameter Δq_μ (or, sometimes, its scalar value $|\Delta q_\mu|$) presents a useful way to visualize the charge distribution in π-systems.

Fig. 6(a) represents the ground state charge alternation functions Δq for a series of 2-azaazulene dyes with $n = 1–5$ performed by *ab initio* method (RHF/6-31G**). It is seen that the shapes of Δq functions for all symmetrical structures are almost insensitive to a length of chromophore: there are constant Δq values along the

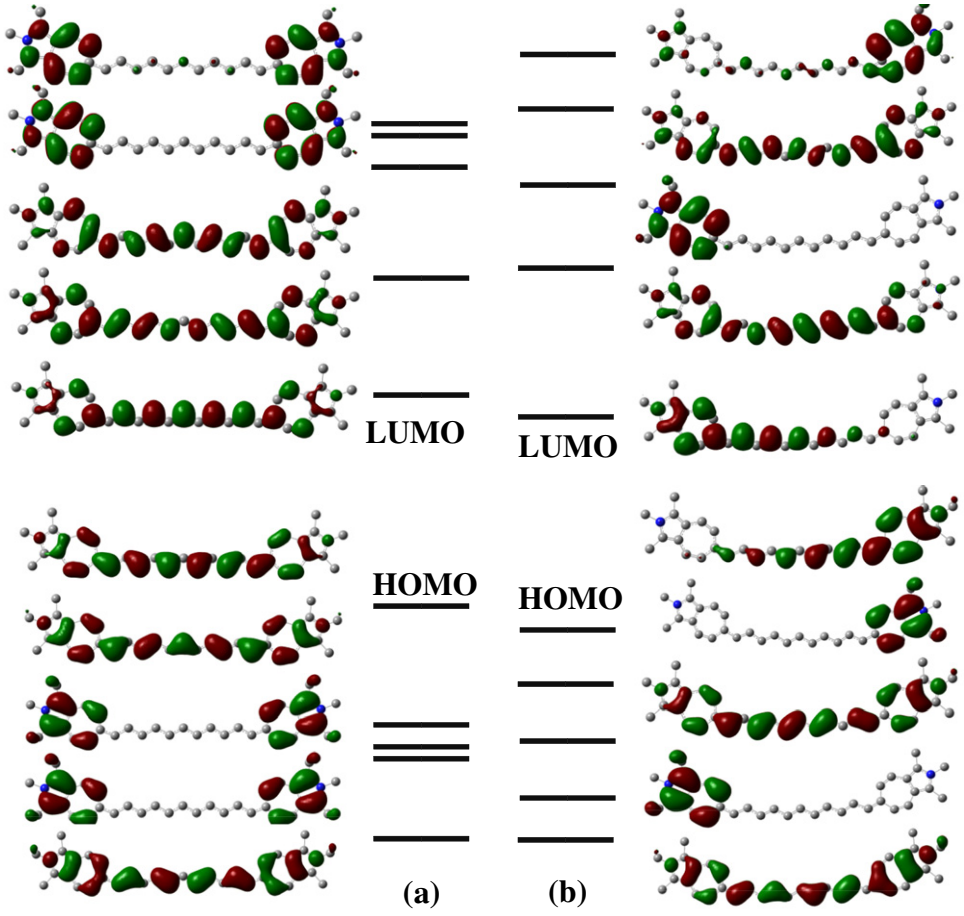

Fig. 4. The shapes and schematic positions of molecular orbitals for symmetrical (a) and asymmetrical (b) forms of 2-azaalulene dye with $n = 5$.

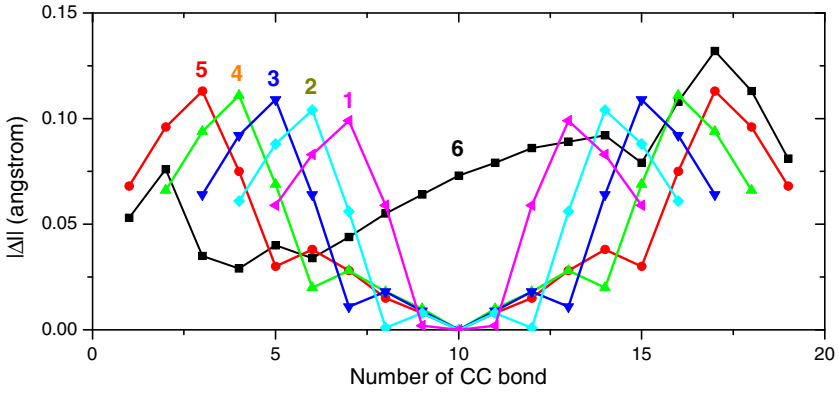

Fig. 5. |Δl| functions for 2-azaalulene dyes with $n = 1$ (curve 1), 2 (curve 2), 3 (curve 3), 4 (curve 4) and 5 (symmetrical form – curve 5; asymmetrical form – curve 6). The bonds numbering corresponds to the longest chain $n = 5$. For comparison, all other molecules are placed into the center. *Ab initio* method (RHF/6-31G**).

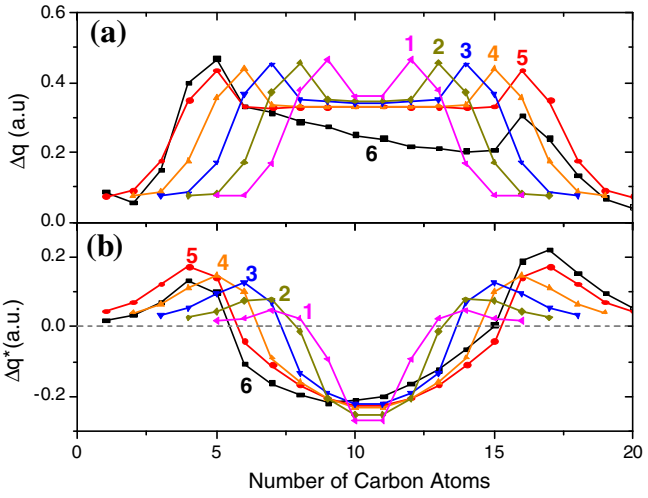

Fig. 6. Δq functions of 2-azaalulene dyes with $n = 1$ (curve 1), 2 (curve 2), 3 (curve 3), 4 (curve 4) and 5 (symmetrical form – curve 5; asymmetrical form – curve 6) in the ground (a) and excited (b) states. The bonds numbering corresponds to the longest chain $n = 5$. For comparison, all other molecules are placed into the center. *Ab initio* method (RHF/6–31G**).

chain, two degenerate maxima at the carbon atoms connecting each terminal residue with the polymethine chain, and essential decrease of Δq values within the terminal groups. Correspondingly, for asymmetrical dye structure at $n = 5$, the Δq function becomes asymmetrical showing a considerable charge changes along the polymethine chain from one terminal group to another.

Fig. 6(b) represents the excited state charge distribution functions Δq^* for a series of 2-azaazulene dyes with $n = 1$–5, while keeping Franck–Condon geometry corresponding to unchanged ground state geometry. It is seen that the molecular backbone can be divided into three parts according to the order of the charge redistribution function after the excitation. Charge alternation within terminal groups is characterized by the same order as the ground state charge alternation, however, with a considerable decrease in charge alternation amplitude. Charge alternation within the polymethine chain is characterized by the opposite order as compare to the ground state Δq function and also smaller charge alternation magnitude similar to traditional polymethine dyes [32]. It is important to compare the ground- and excited state charge distributions for asymmetrical form (dye with $n = 5$). If a ground state Δq function shows an asymmetrical behavior with a considerable change along the chain from one terminal group to another (Fig. 6(a), curve 6), the excited state Δq^* function (Fig. 6(b), curve 6) is almost symmetrical. In summary, we can conclude that after the excitation, the difference between asymmetrical and symmetrical forms becomes much smaller. This effect of excited state symmetrization is confirmed experimentally by the narrow fluorescence shapes which are independent on the solvent polarity (see Fig. 1(b)) and is in accord with the theoretical model proposed by F. Terenziani and A. Painelli for quadrupolar chromophores [33,34].

3.5. Electronic transitions

Based on *ab initio*-optimized geometries, the electronic transitions for a vinylogous series of 2-azaazulene dyes with $n = 1$–5 were evaluated by coupling the semiempirical ZINDO Hamiltonian to a single configuration interaction (SCI) scheme [35]. The SCI active space involves the configurations generated by the promotion of an electron from one of the highest occupied levels to one of the lowest unoccupied levels accordingly to the standard Gaussian procedure. Fig. 7 schematically explains the formation of three following types of electronic transitions based on the different nature of MOs.

The first type includes transitions between two *delocalized MOs*. In Fig. 7 first type of transitions is schematically presented by the promotion of the electron from the *donor* HOMO to LUMO; from the *donor* HOMO to LUMO+1, and from the *donor* HOMO−3 to LUMO. The second type includes transitions between one *local* and one *delocalized* MOs, which is schematically presented by promotion of electron from the *local* HOMO−1 and HOMO−2 to LUMO, and from the *delocalized* HOMO to the *local* LUMO+2 and LUMO+3. The third type involves transitions between the *local* MOs only, schematically presented by promotion of the electron from the *local* HOMO−1 and HOMO−2 to the *local* LUMO+2 and LUMO+3. Symmetry of the MOs, involving corresponding transition, determines the transition oscillator strength and thus, the transition dipole moment.

This definition into three types of electronic transitions is general for many polymethine-like dyes and can be used to explain the sensitivity of transition energies to the length of the polymethine chain *n*. For example, the energies of the transitions involving totally *delocalized* MOs strongly depend on *n*, and decrease regularly upon the lengthening of the chain, whereas the energies of the *local* transitions remain almost unchanged at any length of the polymethine chromophore. This conclusion is important, from one side, for understanding the weaknesses and limitations of quantum chemical theories in calculation of transitions energies,

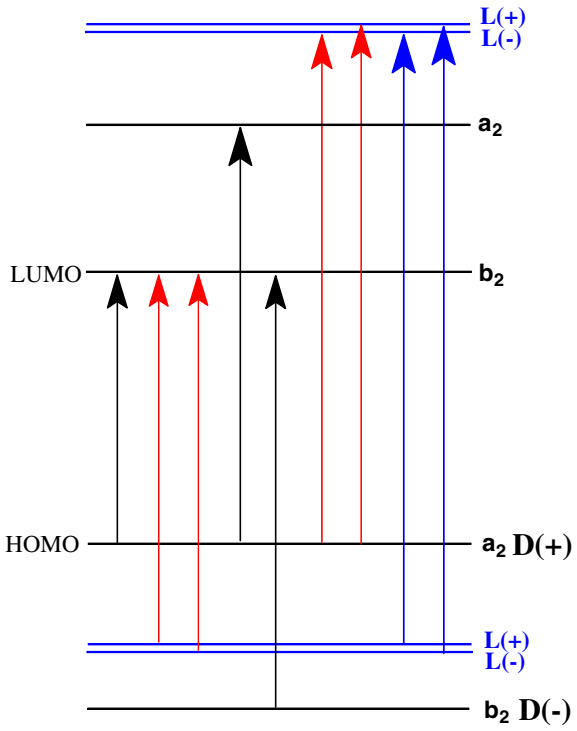

Fig. 7. Schematic of electron promotion between MOs of different types for 2-azaazulene dye with $n = 3$. Arrow indicates a pair of MOs involved into formation of particular transition: black – between *delocalized* orbitals, red – between one *local* and one *delocalized* orbitals, and blue – between two *local* orbitals. D(+) and D(−) are two split *donor* orbitals; L(+) and L(−) are two split *local* orbitals. See explanation in the text. (For interpretation of the references to colour in this figure legend, the reader is referred to the web version of this article.)

Table 2
Combined experimental and calculated results for electronic transitions in 2-azaazulene dye with $n = 3$. ZINDO-SCI calculations, Gaussian 2003.

Transitions	Spectral range (nm)	Transition dipole moments (Debye)	Symmetry of the initial and final states	Main configurations
$S_0 \rightarrow S_1$	800–1100	21.5[a]	$A_1 \rightarrow B_1$	$\|S_1\rangle = 0.95\|H \rightarrow L\rangle$
$S_0 \rightarrow S_2$	600–700	1.4	$L(-) \rightarrow B_1$	$\|S_2\rangle = 0.85\|H\text{-}2 \rightarrow L\rangle$
$S_0 \rightarrow S_3$	600–700	2.8	$L(+) \rightarrow B_1$	$\|S_3\rangle = 0.83\|H\text{-}1 \rightarrow L\rangle$
$S_0 \rightarrow S_4$	520–550	4.2	$A_1 \rightarrow A_1(-)$ mixed	$\|S_4\rangle = 0.68\|H\text{-}3 \rightarrow L\rangle$ $-0.66\|H \rightarrow L{+}1\rangle$
$S_0 \rightarrow S_5$	450–480	1.7	$A_1 \rightarrow A_1(+)$ mixed	$\|S_5\rangle = 0.66\|H\text{-}3 \rightarrow L\rangle$ $+0.70\ \|H \rightarrow L{+}1\rangle$
$S_0 \rightarrow S_6$	400–440	0.26	$A_1 \rightarrow L(-)$	$\|S_6\rangle = 0.78\|H \rightarrow L{+}2\rangle$
$S_0 \rightarrow S_7$	400–440	1.2	$A_1 \rightarrow L(+)$	$\|S_7\rangle = 0.85\|H \rightarrow L{+}3\rangle$

[a] Experimental value for JB17-08 ($n = 3$) equals 18 D in DCM.

and from other side, motivates the further development of the theoretical methods.

Based on the calculated characteristics of the electronic transitions and performing a direct comparison with the spectral measurements for the 2-azaazulene dye with $n = 3$, we present the results in Table 2. The first "cyanine-like" $S_0 \rightarrow S_1$ transition corresponds to typical allowed and almost pure transition between *delocalized* HOMO and LUMO orbitals. Two next transitions, $S_0 \rightarrow S_2$ and $S_0 \rightarrow S_3$, occurring from the *local* HOMO−1 and HOMO−2 to *delocalized* LUMO, are also pure; however they are much less intensive than $S_0 \rightarrow S_1$ transition. To our understanding, these two transitions display themselves in excitation anisotropy spectrum (Fig. 2(a)) as a small valley in the range of 600–700 nm with the angle ≈30° between the absorption and emission transition dipoles. Two next transitions, $S_0 \rightarrow S_4$ and $S_0 \rightarrow S_5$, are mixed and correspond to linear combinations of two almost equal contributions from HOMO−3 → LUMO and HOMO → LUMO+1. Both transitions occur between *delocalized* orbitals. One of them, $S_0 \rightarrow S_4$, is characterized by larger oscillator strength and presumably corresponds to experimentally observed absorption band at 530–540 nm and seen as a flat shoulder in the anisotropy spectrum (Fig. 2(a)). The next, $S_0 \rightarrow S_5$ transition, has a much smaller oscillator strength and, most likely, corresponds to a deepest valley in the excitation anisotropy spectrum in the range of 450–480 nm with the angle ≈65° between absorption and emission transition dipoles. Two next transitions, $S_0 \rightarrow S_6$ and $S_0 \rightarrow S_7$, are pure and correspond to transition from *delocalized* HOMO to *local* LUMO+2 and LUMO+3, respectively. From our calculations, the nature of the so called "blue" fluorescence, shown in Fig. 2(b), is connected with the radiative transition from the *local* LUMO+3 orbital.

Thus, performed investigations have advanced our understanding of the nature of electronic transitions and the structure–property relations in a series of NIR polymethine molecules, which is extremely important for understanding the nonlinear optical behavior of these dyes and their associated nonlinear optical applications to be discussed in our next paper.

4. Conclusions

Spectral-luminescence investigations were performed along with comprehensive quantum chemical analysis of the nature of the electronic transitions in a series of 2-azaazulene dyes with different polymethine chain lengths.

1. All 2-azaazulene dyes show a remarkably large red shift of their main absorption bands at relatively short lengths of the polymethine chain. Even at $n = 1$ the absorption peak reaches 825 nm, which is ≈270 nm longer than traditional polymethine dyes of the same chain length with indolium or thiazolium terminal groups. The effect of 2-azaazulene terminal groups is equivalent to the extension of the polymethine chain to approximately 3 vinylene groups. Note that 2-azaazulene terminal groups give only a slightly smaller (≈30–40 nm) red shift than corresponding polymethine dyes with dihydrobenzo[cd]furo[2,3-f]indolium terminal groups, studied by us earlier [8].
2. All 2-azaazulene dyes demonstrate very small fluorescence (quantum yield is ⩽0.05) and, correspondingly, short fluorescence lifetimes (⩽30 ps, estimated by Strickler–Berg equation [23], and measured by femtosecond pump–probe technique). Two dyes with $n = 1$ and $n = 3$ show very weak but observable fluorescence from the higher excited states, so called "blue" fluorescence in the range 450–550 nm.
3. Symmetry breaking effect is observed experimentally at $n = 3$ (in the polar solvents) and theoretically at $n = 5$ (in a vacuum) giving evidence for the appearance of the asymmetrical molecular structure with BLA.
4. Quantum chemical analysis allows concluding that there are *two types* of molecular orbitals in 2-azaazulene molecules: *local MOs* with the charge mainly localized within terminal groups and *delocalized MOs* with the charge delocalized within the whole molecule. Among *delocalized orbitals*, especially important are two *donor orbitals*, whose energy positions are determined by donor strength of the terminal groups.
5. Based on symmetry and charge distribution within molecular orbitals, *three* following *types* of the electronic transitions may be considered. First type corresponds to transitions between *delocalized MOs*. Second type corresponds to transitions between one *local* and one *delocalized MOs*, and the third type involves the transitions between *local* MOs only. This definition

is important for predicting the sensitivity of the electronic transitions to the length of the polymethine chain *n*. Thus, the energies of the transitions involving totally *delocalized* MOs strongly depend on *n*, and their energies decrease regularly upon the lengthening of the chain, whereas the energies of the *local* transitions remain almost unchanged at any length of the polymethine chromophore.

Acknowledgements

This work is supported by ARO 50372-CH-MUR, DARPA ZOE W31R4Q-09-1-0012, and AFOSR MURI FA9550-10-1-0558.

References

[1] A. Mishra, R.K. Behera, P.K. Behera, B.K. Mishra, G.B. Behera, Chem. Rev. 100 (2000) 1973.
[2] F. Meyers, S.R. Marder, J.W. Perry, Introduction to the nonlinear optical properties of organic materials, in: L.V. Interrante, M.J. Hampden-Smith (Eds.), Chemistry of Advanced Materials: An Overview, Wiley-VCH, New York, 1998.
[3] J. Fabian, H. Nakazumi, M. Matsuoka, Chem. Rev. 92 (1992) 1197.
[4] N. Peyghambarian, L. Dalton, A. Jen, B. Kippelen, S.R. Marder, R. Norwood, J.W. Perry, Laser Focus World 42 (2006) 85.
[5] T.D. Iordanov, J.L. Davis, A.E. Masunov, A. Levenson, O.V. Przhonska, A.D. Kachkovski, Int. J. Quantum Chem. 109 (2009) 3592.
[6] J.M. Hales, J. Matichak, S. Barlow, S. Ohira, K. Yesudas, J.-L. Brédas, J.W. Perry, S.R. Marder, Science 327 (2010) 1485.
[7] O.V. Przhonska, S. Webster, L.A. Padilha, H. Hu, A.D. Kachkovski, D.J. Hagan, E.W. Van Stryland, Two-photon absorption in near-IR conjugated molecules: design strategy and structure–property relations, in: A.P. Demchenko, (Ed.), Advanced Fluorescence Reporters in Chemistry and Biology I: Fundamentals and Molecular Design, Springer Series in Fluorescence, Springer-Verlag, Berlin Heidelberg, 2010.
[8] S. Webster, L.A. Padilha, H. Hu, O.V. Przhonska, D.J. Hagan, E.W. Van Stryland, M.V. Bondar, I.G. Davydenko, Y.L. Slominsky, A.D. Kachkovski, J. Lumin. 128 (2008) 1927.
[9] L.A. Padilha, S. Webster, H. Hu, O.V. Przhonska, D.J. Hagan, E.W. Van Stryland, M.V. Bondar, I.G. Davydenko, Y.L. Slominsky, A.D. Kachkovski, Chem. Phys. 352 (2008) 97.
[10] R.S. Lepkowicz, O.V. Przhonska, J.M. Hales, J. Fu, D.J. Hagan, E.W. Van Stryland, M.V. Bondar, Y.L. Slominsky, A.D. Kachkovski, Chem. Phys. 305 (2004) 259.
[11] J.S. Craw, J.R. Reimers, G.B. Bacskay, A.T. Wong, N.S. Hush, Chem. Phys. 167 (1992) 77.
[12] J.S. Craw, J.R. Reimers, G.B. Bacskay, A.T. Wong, N.S. Hush, Chem. Phys. 167 (1992) 101.
[13] L.M. Tolbert, X. Zhao, J. Am. Chem. Soc. 119 (1997) 3253.
[14] W.P. Su, J.R. Schrieffer, A.J. Heeger, Phys. Rev. Lett. 42 (1979) 1698.
[15] J. Fabian, H. Hartmann, Dyes Pigments 79 (2008) 126.
[16] J. Fabian, Dyes Pigments 84 (2010) 36.
[17] J. Bricks, A. Ryabitskii, A. Kachkovskii, Eur. J. Org. Chem. 2009 (2009) 3439.
[18] J. Bricks, A. Ryabitskii, A. Kachkovskii, Chem. Eur. J. 16 (2010) 8773.
[19] A.B. Ryabitskii, J.L. Bricks, A.D. Kachkovskii, V.V. Kurdyukov, J. Mol. Struct. 1007 (2012) 52.
[20] J.R. Lakowicz, Principle of Fluorescence Spectroscopy, second ed., Kluwer Academic/Plenum Publisher, New York, 1999.
[21] A.B. Ryabitsky, A.D. Kachkovski, O.V. Przhonska, J. Mol. Struct. Theochem. 80 (2) (2007) 75.
[22] J. Fu, L.A. Padilha, D.J. Hagan, E.W. Van Stryland, O.V. Przhonska, M.V. Bondar, Y.L. Slominsky, A.D. Kachkovski, J. Opt. Soc. Am. B 24 (2007) 56.
[23] S. Strickler, R. Berg, J. Chem. Phys. 37 (1962) 814.
[24] O.V. Przhonska, D.J. Hagan, E. Novikov, R. Lepkowicz, E.W. Van Stryland, M.V. Bondar, Y.L. Slominsky, A.D. Kachkovski, Chem. Phys. 273 (2001) 235.
[25] R.S. Lepkowicz, C.M. Cirloganu, O.V. Przhonska, D.J. Hagan, E.W. Van Stryland, M.V. Bondar, Y.L. Slominsky, A.D. Kachkovski, E.I. Mayboroda, Chem. Phys. 306 (2004) 171.
[26] M.J. Frisch, G.W. Trucks, H.B. Schlegel, G.E. Scuseria, M.A. Robb, J.R. Cheeseman, J.A. Montgomery Jr., T. Vreven, K.N. Kudin, J.C. Burant, M. Millam, S.S. Iyengar, J. Tomasi, V. Barone, B. Mennucci, M. Cossi, G. Scalmani, N. Rega, G.A. Petersson, H. Nakatsuji, M. Hada, M. Ehara, K. Toyota, R. Fukuda, J. Hasegawa, M. Ishida, T. Nakajima, Y. Honda, O. Kitao, H. Nakai, M. Klene, X. Li, J.E. Knox, H.P. Hratchian, J.B. Cross, C. Adamo, J. Jaramillo, R. Gomperts, R.E. Stratmann, O. Yazyev, A.J. Austin, R. Cammi, C. Pomelli, J.W. Ochterski, P.Y. Ayala, K. Morokuma, G.A. Voth, P. Salvador, J.J. Dannenberg, V.G. Zakrzewski, S. Dapprich, A.D. Daniels, M.C. Strain, O. Farkas, D.K. Malick, A.D. Rabuck, K. Raghavachari, J.B. Foresman, J.V. Ortiz, Q. Cui, A.G. Baboul, S. Clifford, J. Cioslowski, B.B. Stefanov, G. Liu, A. Liashenko, P. Piskorz, I. Komaromi, R.L. Martin, D.J. Fox, T. Keith, M.A. Al-Laham, C.Y. Peng, A. Nanayakkara, M. Challacombe, P.M.W. Gill, B. Johnson, W. Chen, M.W. Wong, C. Gonzalez, J.A. Pople, GAUSSIAN 03, Revision B.05, Gaussian Inc., Pittsburgh PA, 2003. 1–20.
[27] R. Radeglia, J. Prakt. Chem. 315 (1973) 1121.
[28] G. Bach, S. Daehne, Cyanine dyes and related compounds, in: M. Sainsbury (Ed.), Rodd's Chemistry of Carbon Compounds, 2nd Supplements to, second ed., Elsevier Science, Amsterdam, 1997, p. 383.
[29] S. Dähne, Science 199 (1978) 1163.
[30] A.D. Kachkovskii, Russ. Chem. Rev. 66 (1997) 715.
[31] S. Webster, J. Fu, L.A. Padilha, O.V. Przhonska, D.J. Hagan, E.W. Van Stryland, M.V. Bondar, Y.L. Slominsky, A.D. Kachkovski, Chem. Phys. 348 (2008) 143.
[32] O.D. Kachkovski, D.A. Yushchenko, G.O. Kachkovski, N.V. Pilipchuk, Dyes Pigments 66 (2004) 223.
[33] F. Terenziani, A. Painelli, C. Katan, M. Charlot, M. Blanchard-Desce, J. Am. Chem. Soc. 128 (2006) 15742.
[34] F. Terenziani, O.V. Przhonska, S. Webster, L.A. Padilha, Y.L. Slominsky, I.G. Davydenko, A.O. Gerasov, Y.P. Kovtun, M.P. Shandura, A.D. Kachkovski, D.J. Hagan, E.W. Van Stryland, A. Painelli, J. Phys. Chem. Lett. 1 (2010) 1800.
[35] A. Tomlinson, D. Yaron, J. Comput. Chem. 24 (2003) 1782.